



DØnote 4832-CONF

## Search for Direct Production of Scalar Bottom Quarks with the DØ Detector in $p\bar{p}$ Collisions at $\sqrt{s} = 1.96$ TeV

The DØ Collaboration  
URL <http://www-d0.fnal.gov>

(Dated: June 28, 2005)

A search for direct production of scalar bottom quarks ( $\tilde{b}$ ) is performed with  $310 \text{ pb}^{-1}$  of data collected by the DØ experiment in  $p\bar{p}$  collisions at  $\sqrt{s} = 1.96$  TeV at the Fermilab Tevatron. The topologies analyzed consist of two  $b$  jets and an imbalance in transverse momentum due to neutralinos ( $\tilde{\chi}_1^0$ ), with  $\tilde{\chi}_1^0$  assumed to be the lightest supersymmetric particle (LSP). We find our data consistent with standard model expectations, and set a 95% CL limit in the  $(m_{\tilde{b}}, m_{\tilde{\chi}_1^0})$  mass plane, improving significantly upon the results from Run I of the Tevatron.

*Preliminary Results for Summer 2005 Conferences*

## I. INTRODUCTION

This analysis searches for the pair production of scalar bottom quarks ( $\tilde{b}$ ) at the Tevatron at  $\sqrt{s} = 1.96$  TeV that subsequently decay into bottom quarks and the lightest neutralino ( $\tilde{\chi}_1^0$ ), taken as the lightest supersymmetric particle (LSP):  $\tilde{b} \rightarrow b + \tilde{\chi}_1^0$ . The topology of the events for this process corresponds to a final state with two acoplanar  $b$  jets and missing transverse energy ( $\cancel{E}_T$ ) due to undetected neutralinos.

## II. DATA SAMPLE

This study is performed on data collected with the DØ detector [1] during the Run II of the Fermilab Tevatron. The data sample corresponds to two triggers (MHT30\_3CJT5 then replaced by JT1\_ACO\_MHT\_HT), which have been specifically designed for  $\cancel{E}_T$  + jets topologies. If we define  $\cancel{H}_T = |\sum_{\text{jets}} \vec{p}_T|$  and  $H_T = \sum_{\text{jets}} |\vec{p}_T|$ , the vectorial and scalar sum of the jet transverse momenta, the conditions for MHT30\_3CJT5 are:

- At Level 1 (L1): CJT(3,5) - at least 3 trigger towers with  $E_T > 5$  GeV (a trigger tower spans regions of azimuth and pseudo-rapidity  $\Delta\phi \times \Delta\eta = 0.2 \times 0.2$  [1], [2])
- At Level 2 (L2):  $\cancel{H}_T > 20$  GeV
- At Level 3 (L3):  $\cancel{H}_T > 30$  GeV

and the conditions for JT1\_ACO\_MHT\_HT are:

- L1: CJT(3,5) - at least 3 trigger towers with  $E_T > 5$  GeV
- L2:  $\cancel{H}_T > 20$  GeV, *Acoplanarity*  $< \frac{15}{16}\pi$
- L3:  $\cancel{H}_T > 30$  GeV, *Acoplanarity*  $< 170^\circ$ ,  $H_T > 50$  GeV

where the *Acoplanarity* is defined as the difference in azimuthal angle  $\Delta\phi$  between the 2 leading jets [2].

An event preselection is performed to reduce the data sample to a manageable size by requiring events with  $\cancel{H}_T > 40$  GeV,  $\cancel{E}_T > 40$  GeV, and more than 1 jet. The purpose of the  $\cancel{H}_T$  and  $\cancel{E}_T$  criteria is to stay away from values where the trigger is inefficient.

After removing bad runs and bad luminosity blocks we retain a total integrated luminosity of about  $310 \text{ pb}^{-1}$  (starting from about 37 millions triggered events, we end up with 827,517 events).

A “good jet” is different from the standard jet used in DØ. The jets we start with are reconstructed with the Run II cone algorithm of radius  $R = \sqrt{(\Delta\phi)^2 + (\Delta\eta)^2} = 0.5$ . All the standard good jet criteria are used, except the upper cutoff at 0.95 on the electromagnetic fraction (EMF). Jet Energy Scale (JES) corrections are applied to all good jets, except for those with  $\text{EMF} > 0.90$ , and for those that are matched to a good electromagnetic (EM) object. The induced changes are propagated to the  $\cancel{E}_T$  accordingly. The reason for this procedure is to prevent the enhancement of  $\cancel{E}_T$  from JES corrections that are determined for typical jets, but overestimate energies of jets with large electromagnetic fractions.

Events with obvious presence of calorimeter noise, and events with at least one “bad jet” (failing the jet quality selection) with  $p_T > 15$  GeV are removed. The overall efficiency of these final criteria is estimated from data (“zero bias” and events with two jets emitted back-to-back) to be 96.1%.

## III. SIMULATION OF SIGNAL

The signal is simulated in the framework of a generic MSSM in which we only vary the masses of the lightest scalar bottom quark ( $\tilde{b}_1$ ) and the lightest neutralino ( $\tilde{\chi}_1^0$ ) taken as the LSP. The signal is generated using PYTHIA 6.202 [3] with CTEQ5L parton density functions [4]. The  $\tilde{b}_1$  squark is forced to decay into a  $b$  quark and a  $\tilde{\chi}_1^0$ . A full GEANT-3 [5] simulation of the DØ detector is performed with an average of 0.8 min-bias events overlayed. To simplify notations, in what follows,  $\tilde{b}_1$  is simply referred to as “sbottom” or “scalar bottom quark” ( $\tilde{b}$ ).

Since, at the Tevatron, scalar bottom quarks are produced in the same way and with the same cross section as scalar top quarks, we calculate the NLO sbottom production cross section as a function of the sbottom mass using PROSPINO-2 [6]. The result is displayed as the center thick curve in Fig. 1-(a). The two outer thinner curves correspond to the cross section calculated with the renormalization and factorization scales kept equal but varied by a factor 2 (upper one) and a factor 0.5 (lower one) respectively. The corresponding relative uncertainty on the cross section as a function of the sbottom mass is shown in Fig. 1-(b). The NLO production cross section drops from about 10 pb at low masses down to about 0.1 pb at high masses.

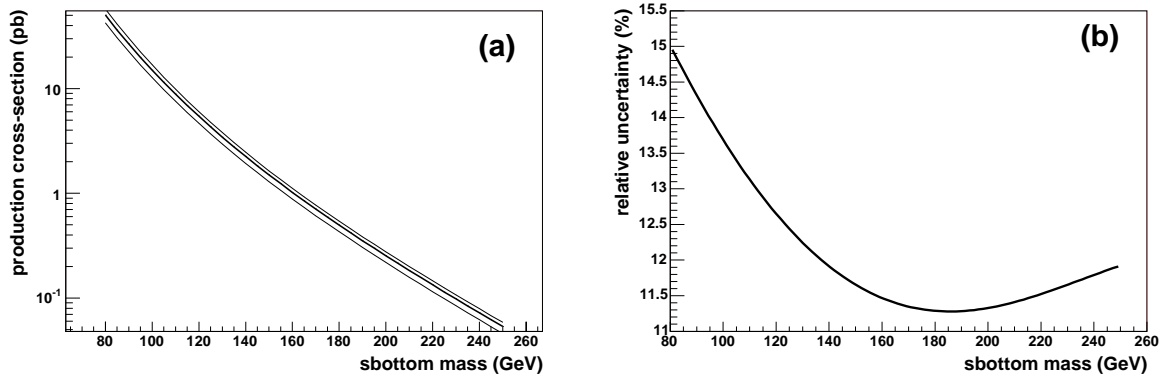


FIG. 1: (a) Prospino NLO  $\tilde{b}\tilde{b}$  pair production cross section (thick central line) as a function of  $m_{\tilde{b}}$  at the Tevatron Run II. The two outer thinner lines correspond to a change in both the renormalization and factorization scales by a factor 2 (upper one) and a factor 0.5 (lower one) respectively. (b) Corresponding relative uncertainty.

In general, for relatively small sbottom masses ( $m_{\tilde{b}} \sim 100$  GeV), the mean  $\cancel{E}_T$  and jet  $p_T$  are relatively small and close to what is measured in  $W/Z$  + jets and  $t\bar{t}$  events, but they become substantially larger for higher sbottom masses. For instance, for  $m_{\tilde{\chi}_1^0} = 70$  GeV and for  $m_{\tilde{b}}$  varying from 100 to 160 GeV, the mean  $\cancel{E}_T$  varies from 30 to 75 GeV and the leading jet mean  $p_T$  varies from 40 to 85 GeV/c.

#### IV. BACKGROUNDS FROM STANDARD-MODEL PROCESSES

The standard model (SM) backgrounds relevant to our analysis comprise weak bosons and di-bosons decaying leptonically, produced together with jets, and  $t\bar{t}$  decaying into the lepton +jets or dilepton channels. These processes were generated with ALPGEN [7] interfaced with PYTHIA. The parton density function used is again CTEQ5L. The scale  $Q$  chosen for the hard process is  $Q^2 = M_{W/Z}^2 + \sum m_T^2$  [7]. A full simulation of the detector is used, and again 0.8 min-bias events on average are overlayed.

To estimate the backgrounds coming from  $W/Z$  + jets processes, a K-factor is derived by comparing the LO and NLO cross sections computed with MCFM [8] which is then multiplied by the LO ALPGEN cross section. To estimate the  $t\bar{t}$  contribution, the theoretical NLO  $t\bar{t}$  production cross section ( $6.77 \pm 0.42$  pb [9]) and branching ratios are used. The results are displayed in Table I. A systematic uncertainty of 15% is applied on the NLO SM cross sections.

#### V. EVENT SELECTION

Table II shows the effect of applying sequentially the analysis criteria to data, signal and background samples. As reference, the signal is taken to correspond to  $[(m_{\tilde{b}}, m_{\tilde{\chi}_1^0}) = (140, 80)$  GeV]. As a first approach, the selections are tuned so to maintain good sensitivity to signal, even for small sbottom masses. In a later section, we show that for larger masses, higher cutoffs on  $\cancel{E}_T$  (C1) and jet  $p_T$  (C4 and C5) can be applied to increase the sensitivity to signal.

Criteria C1-C12 are meant to reduce instrumental and multi-jets backgrounds (they are generically called QCD background in the rest of the paper). The QCD contributions are not evaluated at this stage of the event selection and thus are not included in the column labeled SM in table II, but are discussed in section VIB. In criterion C7.8, CPF is the charged particle fraction of the jet. C4, C5, and C13-C15 are effective on SM backgrounds in general, and C16

TABLE I: Standard-model (SM) processes, number of events generated, LO cross sections in pb from the generator, K-factors and NLO cross sections in pb (from Ref. [8], except for  $t\bar{t}$  which is computed using the NLO cross section from Ref. [9]).

SM process	# evts	$\sigma(\text{LO})$	K-factor	$\sigma(\text{NLO})$
$W(e\nu) + jj$	53500	225	1.28	288
$W(\mu\nu) + jj$	51750	225	1.28	288
$W(\tau\nu) + j$	97750	714	1.18	840
$Z(\tau\tau) + j$	96500	70	1.17	81
$Z(\nu\nu) + jj$	33500	133	1.31	174
$W(\tau\nu) + b\bar{b}$	27250	2.1	2	4.2
$Z(\nu\nu) + b\bar{b}$	98000	1.4	2.3	3.3
$t\bar{t} \rightarrow b\bar{b}l\nu jj$	191300			2.98
$t\bar{t} \rightarrow b\bar{b}l\nu l\nu$	57500			0.74
$WW$ inclusive	50000	8.6	1.31	11.3
$WZ$ inclusive	53000	2.6	1.35	3.5
$ZZ$ inclusive	53500	1.2	1.28	1.5
$WZ \rightarrow e\nu b\bar{b}$	73000	0.043	1.35	0.058
$WZ \rightarrow \mu\nu b\bar{b}$	39500	0.043	1.35	0.058
$ZZ \rightarrow \nu\nu b\bar{b}$	52024	0.064	1.28	0.082

TABLE II: Sequence of criteria applied for the selection, with the corresponding remaining events, together with the signal efficiency, for a signal corresponding to  $(m_b, m_{\tilde{\chi}_1^0}) = (140, 80)$ .

Criterion		events remaining			$\epsilon_{\text{Signal}}$
		Data	SM (no QCD)	Signal	
Preselection:		827517	$61100 \pm 350$	$362 \pm 6$	59%
<b>C1 :</b>	$\cancel{E}_T > 60$ GeV	154452	$16300 \pm 170$	$204 \pm 4$	33%
<b>C2 :</b>	Vertex $ z  < 60$ cm	126974	$16020 \pm 170$	$201 \pm 4$	33%
<b>C3 :</b>	$A_{\text{coplanarity}} < 165^\circ$	82693	$15160 \pm 160$	$189 \pm 4$	31%
<b>C4 :</b>	1st leading jet $p_T > 40$ GeV	80196	$13190 \pm 150$	$178 \pm 4$	29%
<b>C5 :</b>	2nd leading jet $p_T > 15$ GeV	70893	$11870 \pm 140$	$168 \pm 4$	27%
<b>C6 :</b>	$ \eta_{\text{jet1}}^{\text{det}}  < 0.9$	45174	$7200 \pm 110$	$132 \pm 3$	21%
<b>C7_8 :</b>	jet1,2 CPF $> 0.05$	23994	$6250 \pm 100$	$125 \pm 3$	20%
<b>C9_10 :</b>	jet1,2 EMF $< 0.95$	22254	$5170 \pm 90$	$124 \pm 3$	20%
<b>C11 :</b>	Bad jet veto ( $p_T > 15$ GeV)	9672	$5070 \pm 90$	$123 \pm 3$	20%
<b>C12 :</b>	$\Delta_{\text{min}}(\cancel{E}_T, \text{any good jet}) > 35^\circ$	5151	$4270 \pm 85$	$105 \pm 3$	17%
<b>C13 :</b>	Isolated EM veto $p_T > 5$ GeV	4355	$3660 \pm 80$	$104 \pm 3$	17%
<b>C14 :</b>	Isolated muon veto $p_T > 5$ GeV	3745	$3110 \pm 75$	$103 \pm 3$	17%
<b>C15 :</b>	Isolated track veto $p_T > 5$ GeV	1642	$1480 \pm 50$	$78 \pm 2$	13%
<b>C16 :</b>	$Nj = 2, 3$	1433	$1335 \pm 48$	$69 \pm 2$	11%

on  $t\bar{t}$  background specifically. Since we do not expect isolated electrons, muons or taus in signal events, we veto these using **C13**, **C14** and **C15**.

### A. Data versus MC efficiencies

The MC events are corrected for jet reconstruction efficiency relative to data. The  $E_T$  of jets and the  $p_T$  of electrons and muons are smeared in the MC so that resolutions in the MC correspond to resolutions measured in data. The effect of the smearing is propagated to the  $\cancel{E}_T$ .

Since we veto isolated electrons, muons or tracks, any discrepancy in efficiency between data and Monte Carlo in identifying these objects can potentially increase remaining SM backgrounds. An estimated constant 95% data/MC efficiency is assigned to isolated electrons, muons, and single tracks, with an overall systematic uncertainty of 5% (see Section IX).

## VI. RESULTS

### A. Before $b$ tagging

Having applied all the above selections, Table III gives the number of events expected for SM backgrounds, the number of events observed in data, and the number of events expected for a signal corresponding to  $(m_{\tilde{b}}, m_{\tilde{\chi}_1^0}) = (140, 80)$  GeV. Fig. 2 shows the distributions in  $\cancel{E}_T$  and in the  $p_T$  of the leading and next-to leading jets, for data, signal  $[(m_{\tilde{b}}, m_{\tilde{\chi}_1^0}) = (140, 80)$  GeV] and SM backgrounds. There is general good agreement between the SM (shaded histograms) and data (points). The dashed lines show the correlated systematic uncertainties on the SM background. It can also be seen from these plots that the signal is more than one order of magnitude smaller than the background. Since a good fraction of the background corresponds to processes with light flavor jets in their final states, we use  $b$  tagging in the final stage of the analysis in order to significantly increase the signal over background ratio (S/B).

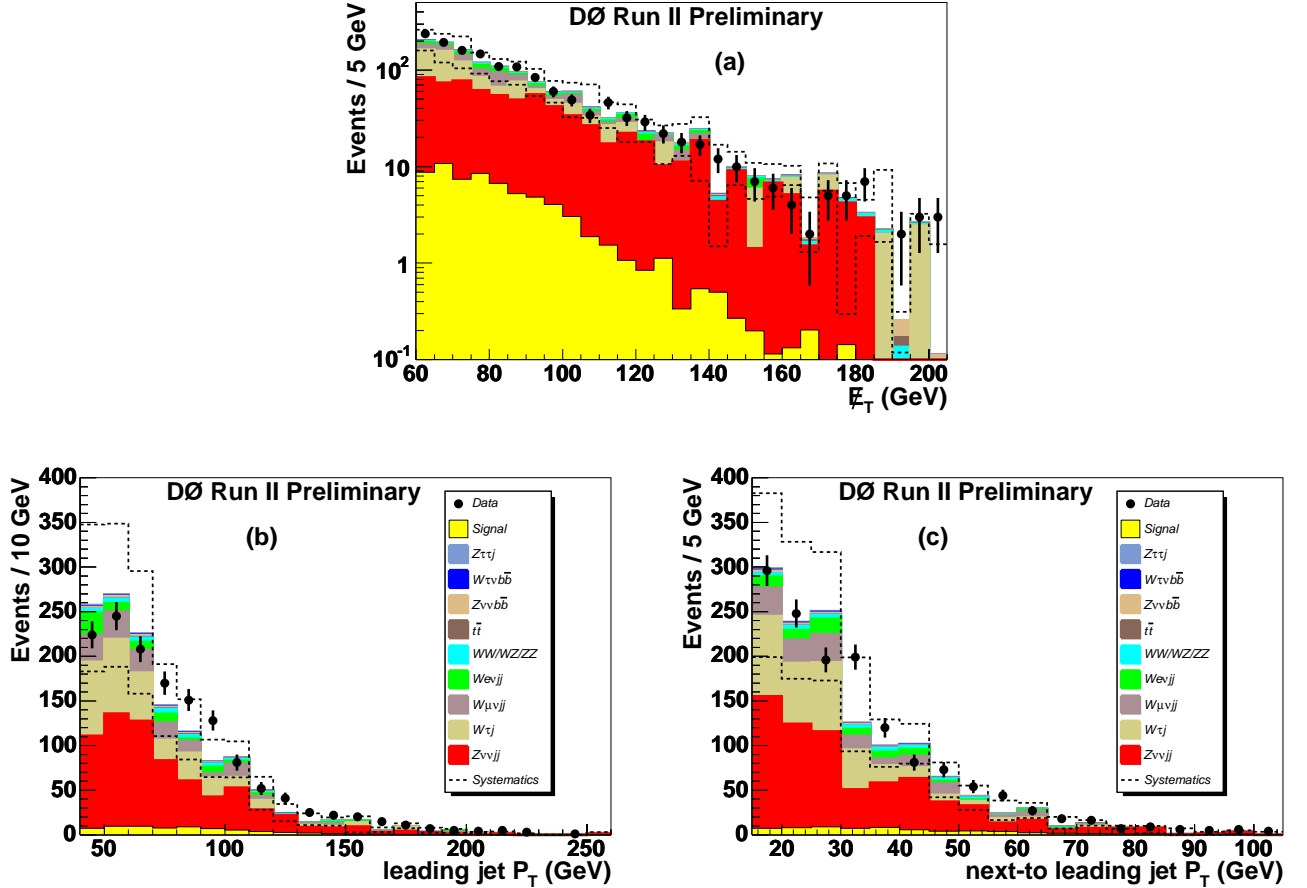


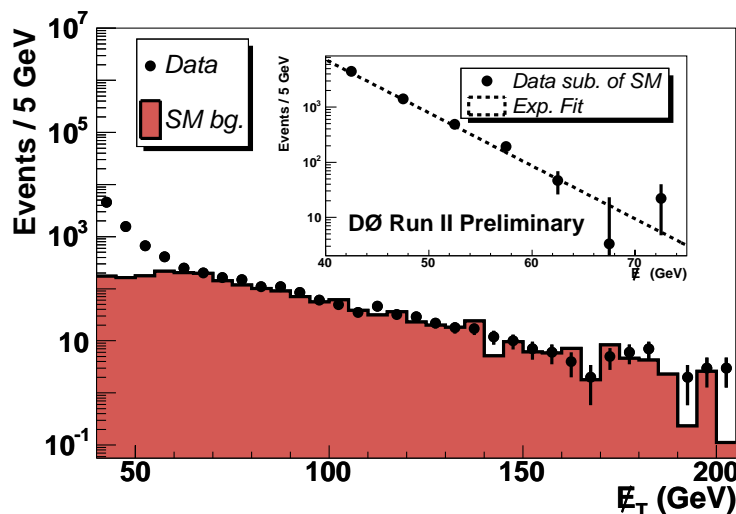
FIG. 2:  $\cancel{E}_T$  (a),  $p_T$  of leading (b) and next-to leading (c) jets after imposing all selection criteria (C1-C16).

### B. Estimate of the QCD background

In order to estimate the QCD background and how much would survive  $b$  tagging, we examined our selected data sample without the criterion on  $\cancel{E}_T$  (C1). Fig. 3 shows that data are well reproduced by the SM background at high  $\cancel{E}_T$ , and we attribute the exponential rise at low  $\cancel{E}_T$  to QCD background. A fit to  $\cancel{E}_T < 60$  GeV after subtraction of the contributions from the SM is shown in the figure insert. When the fit is extrapolated to  $\cancel{E}_T > 60$  GeV, it provides an estimate of 80 QCD events. Since, a priori, these events can be assumed not to be enriched in heavy flavors, we expect that after  $b$ -tagging only a few QCD events will survive. For a  $\cancel{E}_T$  cutoff above 60 GeV, the QCD contribution becomes negligible. This background contribution is thus ignored in the rest of this analysis.

TABLE III: Results after all selection criteria, before and after  $b$ -tagging.

SM process	Events before $b$ tagging	Events after $b$ tagging
$W(e\nu) + jj$	$74 \pm 11$	$1.4 \pm 0.8$
$W(\mu\nu) + jj$	$152 \pm 16$	$2.3 \pm 0.9$
$W(\tau\nu) + j$	$337 \pm 29$	$8.3 \pm 1.6$
$Z(\nu\nu) + jj$	$707 \pm 33$	$11 \pm 2$
$W(\tau\nu) + b\bar{b}$	$5.4 \pm 0.5$	$2.3 \pm 0.2$
$Z(\nu\nu) + b\bar{b}$	$16 \pm 1$	$7.5 \pm 0.2$
$Z(\tau\tau) + j$	$5 \pm 1$	$0.1 \pm 0.1$
$t\bar{t} \rightarrow b\bar{b}l\nu jj$	$4.5 \pm 0.1$	$2.1 \pm 0.1$
$t\bar{t} \rightarrow b\bar{b}l\nu l\nu$	$1.3 \pm 0.1$	$0.7 \pm 0.1$
$WW$ inclusive	$12 \pm 1$	$0.5 \pm 0.1$
$WZ$ inclusive	$11 \pm 1$	$0.5 \pm 0.1$
$ZZ$ inclusive	$8.5 \pm 0.3$	$0.9 \pm 0.06$
$WZ \rightarrow e\nu b\bar{b}$	$0.1 \pm 0.1$	$0 \pm 0$
$ZZ \rightarrow \nu\nu b\bar{b}$	$1.6 \pm 0.1$	$0.8 \pm 0.1$
Total SM	$1335 \pm 48$	$38.6 \pm 2.8$
Data	1433	36
signal for $(m_{\tilde{b}}, m_{\tilde{\chi}_1^0}) = (140, 80)$ GeV	$68.8 \pm 2.3$	$35.0 \pm 1.2$

FIG. 3: Distribution in  $E_T$  after applying all criteria but C1.

## VII. $b$ TAGGING

Since signal events comprise two jets coming from the hadronization of  $b$  quarks, we use the DØ Jet Lifetime Probability (JLIP)  $b$ -tagging algorithm to increase our S/B ratio. This algorithm computes a probability for a jet ( $\eta < 2.5$ ) to be light-flavored, based on the impact parameter of the tracks in the jet. Since the  $b$ -tagging algorithms deal with “taggable” jets, namely those associated with track jets, we first study the “taggability” of jets in the data sample to be able to properly weight events in the MC samples.

### A. JLIP single tag

The JLIP  $b$ -tagger is provided with six certified working points of which we selected the one with the smallest mistag rate ( $\approx 0.1\%$  for jets of  $E_T < 95$  GeV on average) as yielding the best value of  $S/\sqrt{B}$ . At this stage of the analysis we require at least one JLIP  $b$  tag in the event. In what follows, this is referred to as a “single  $b$  tag”.

Because the current full simulation of the tracker does not reproduce sufficiently well enough what is observed in data, the tagging algorithm cannot be applied directly on MC events. In addition to weighting the MC jets for taggability, the different flavors ( $b$ ,  $c$ ,  $\tau$ , light) of taggable jets in an event must also be properly weighted by parameterized Tag Rate Functions (TRF) that are jet  $p_T$  and  $\eta$  dependent.

Using  $Z \rightarrow b\bar{b}$ ,  $Z \rightarrow c\bar{c}$ ,  $Z \rightarrow \tau\tau$ , and  $Z \rightarrow q\bar{q}$  MC samples, we found the taggability for  $b$  jets,  $c$  jets, and  $\tau$  jets relative to light flavored jets, to be 1.03, 1.02 and 0.62, respectively. Since the taggability in data is measured on a sample containing mostly light flavored jets, we correct the taggability used in the analysis by these factors. On the  $Z \rightarrow c\bar{c}$  and  $Z \rightarrow \tau\tau$  MC samples, we checked that the tagging efficiency for  $c$  jets and  $\tau$  jets are the same within 3%.

Table III shows the results after all selections, including single  $b$  tagging, for SM backgrounds, data, and signal corresponding to  $(m_{\tilde{b}}, m_{\tilde{\chi}_1^0}) = (140, 80)$  GeV.

The distributions in the number of jets and in  $\cancel{E}_T$  are displayed in Fig. 4, showing agreement between data and SM backgrounds. The dashed lines show the effect of systematic uncertainties on the SM background. No excess is seen in data relative to SM expectations.

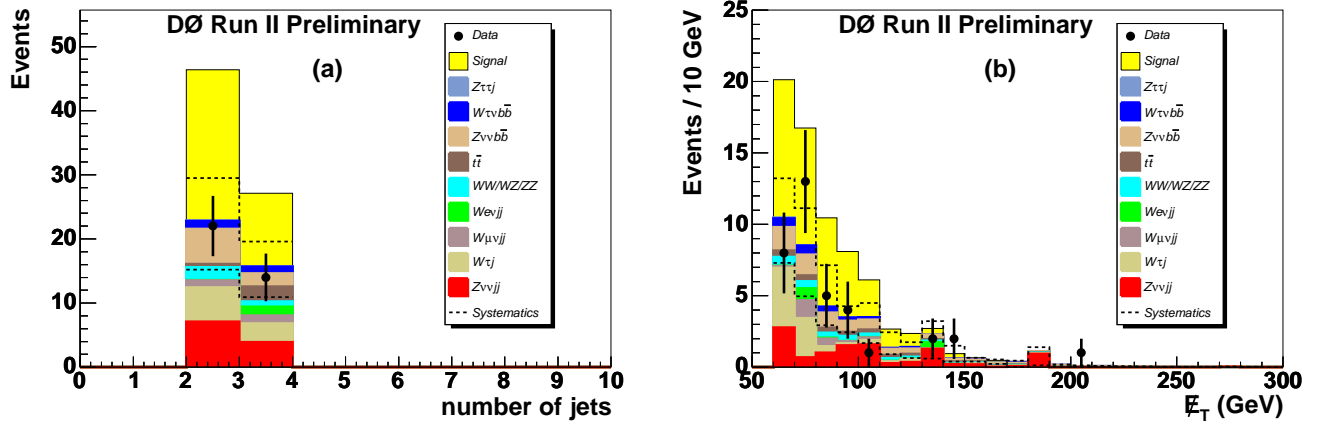


FIG. 4: Number of jets (a) and  $\cancel{E}_T$  (b) after all selections, including single  $b$  tagging, for  $(m_{\tilde{b}}, m_{\tilde{\chi}_1^0}) = (140, 80)$ .

### VIII. OPTIMIZATION FOR HIGH MASSES

As mentioned in Section III, since for higher masses of sbottom the mean  $\cancel{E}_T$  and jet  $p_T$  become substantially larger than expectations from the SM backgrounds, this provides a new lever for improving the sensitivity to signal.

In this work we use three sets of final analysis cutoffs:

- $\cancel{E}_T > 60$  GeV, 1st jet  $p_T > 40$  GeV, 2nd jet  $p_T > 15$  GeV (small masses)
- $\cancel{E}_T > 80$  GeV, 1st jet  $p_T > 40$  GeV, 2nd jet  $p_T > 15$  GeV (medium masses)
- $\cancel{E}_T > 100$  GeV, 1st jet  $p_T > 70$  GeV, 2nd jet  $p_T > 40$  GeV (large masses)

Table IV shows for two high sbottom-mass points, the chosen  $\cancel{E}_T$  and  $p_T$  cutoffs, together with the resulting number of events found after all selections including single  $b$  tagging for data, SM background and signal. No excess is observed in data relative to SM expectations.

TABLE IV: Number of events for different sbottom masses after all selections, including single  $b$  tagging, with **C1**, **C4**, and **C5** optimized for medium and large sbottom mass.

$(m_{\tilde{b}}, m_{\tilde{\chi}_1^0})$ in GeV	(160,75)	(205,60)
<b>C1</b> : $\cancel{E}_T$ [GeV]	80	100
<b>C4</b> : jet 1 $p_T$ [GeV]	40	70
<b>C5</b> : jet 2 $p_T$ [GeV]	15	40
data	15	2
<b>SM</b>	$19.6 \pm 1.7$	$4.40 \pm 0.44$
signal	$21.6 \pm 0.7$	$6.10 \pm 0.17$

## IX. SYSTEMATIC UNCERTAINTIES

The following systematic uncertainties are taken into account in this analysis:

- Luminosity:  $\pm 6.5\%$ .
- The systematics affecting the **SM** background NLO cross sections are taken as  $\pm 15\%$ .
- The systematics affecting the NLO cross sections for signal are evaluated to vary between  $\pm 11\%$  and  $\pm 15\%$  (for  $m_{\tilde{b}}$  in the range 80-250 GeV). This reflects the uncertainties returned by **PROSPINO** ( $< 1\%$ ) and the variations in NLO cross sections when the renormalization and factorization scales are changed by a factor of 2 (see Fig. 1).
- MC statistics: varies, depending upon the final selections and the mass points (for signal), these can reach  $\pm 10\%$  for the contributions from the **SM** and  $\pm 5\%$  for signal.
- JES: found by changing the JES by  $\pm 1$  s.d., where s.d. are the JES uncertainties (standard deviations) on data and MC added in quadrature, resulting in  $^{+13.8}_{-22.3}\%$  relative uncertainty on the prediction for the **SM** background, and  $^{+15.7}_{-12.1}\%$  relative uncertainty on the signal.
- Jet ID reconstruction efficiency: found by changing by  $\pm 1$  s.d. the efficiency parameterizations, resulting in  $^{+3.8}_{-3.7}\%$  on **SM** and  $^{+3.4}_{-3.3}\%$  on signal.
- Taggability: found by changing by  $\pm 1$  s.d. the taggability parameterizations, resulting in  $\pm 3.7\%$  on **SM** and  $\pm 3.2\%$  on signal.
- $b$  tagging: found by changing by  $\pm 1$  s.d. the  $b$ -tagging efficiency, resulting in  $^{+8.4}_{-8.3}\%$  on **SM** and  $^{+7.0}_{-7.1}\%$  on signal.
- $\tau$  jets:  $\pm 5\%$  is used to account for the uncertainty on the taggability and tagging for  $\tau$  jets.
- Trigger: past trigger studies have shown that after offline selections, the trigger efficiency is  $\approx 100\%$ . We take a  $\pm 5\%$  uncertainty on trigger efficiency for **SM** and for signal.
- Isolated-lepton ID efficiency: see discussion in Section V A. Switching on a 95% data/MC relative efficiency for isolated electrons, muons and single tracks, increases the background after all selections (including  $b$  tagging) by 5%. We therefore use a  $\pm 5\%$  systematic uncertainty on these efficiencies.

## X. LIMITS

Since we do not observe any excess in data relative to expectations from **SM** background, we set limits on the production of scalar bottom quarks at the Tevatron. Using the number of events found after all selections (including  $b$  tagging) for data, **SM** background and signal, the 95% CL (confidence level) limits are obtained using a  $CL_s$  approach [10] with correlations among systematic uncertainties taken into account. For signal, systematics due to theory are not included in the  $CL_s$  calculation, from which a coefficient for exclusion is derived. The coefficient is multiplied by the theoretical cross section for the given sbottom mass to obtain the excluded production cross section at the 95% CL. Taking account of the systematics on the cross section for signal, the mass limits are derived by intersecting the 95% CL excluded cross section curve, as a function of mass, with the smaller NLO cross section value given by **PROSPINO** for which both the renormalization and factorization scales have been changed by a factor of two (see Fig. 1 for details).



The effect on sensitivity of the three sets of selections described in Section VIII is illustrated in Fig. 5. The plots show, for  $m_{\tilde{\chi}_1^0} = 60$  GeV, the excluded cross section (thickest line) at the 95% CL compared to the PROSPINO cross section (see Fig. 1 for details) as a function of  $m_{\tilde{b}}$ , for the three sets of  $(\cancel{E}_T, p_{T1}, p_{T2})$  cutoffs (a)-(c), and for their combined values (d).

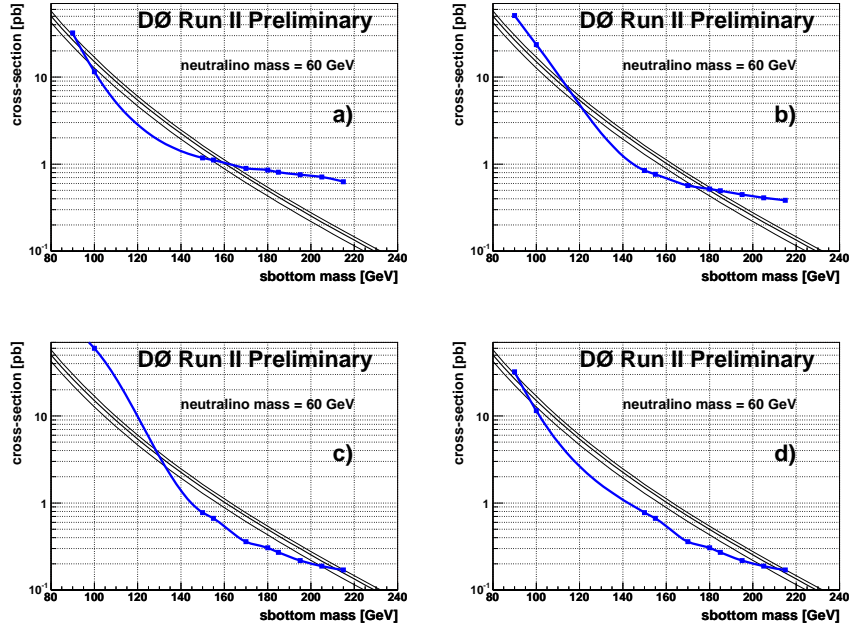


FIG. 5: Excluded cross sections (thickest line) at the 95% CL compared to theory for  $m_{\tilde{\chi}_1^0} = 60$  GeV, and for the set of cutoffs on  $(\cancel{E}_T, p_{T1}, p_{T2})$ : (a) (60, 40, 15), (b) (80, 40, 15), and (c) (100, 70, 40). Their combined effect is given in (d).

The preliminary results of this analysis are summarized in the 95% CL exclusion contour plot displayed in Fig. 6, showing a significant improvement on previous measurements.

## XI. CONCLUSIONS AND PERSPECTIVES

This analysis is the first one performed in Run II of the Tevatron to search for the pair production of scalar bottom quarks. The exclusion contour we obtain is substantially more restrictive than the ones published with Run I Tevatron data. Nevertheless, there is still some room for further improvement for instance, a better optimization of the  $\cancel{E}_T$  and jet  $p_T$  cutoffs, consideration of double  $b$  tagging to increase sensitivity even further, and reduction of systematic uncertainty on the jet energy scale.

## Acknowledgments

We thank the staffs at Fermilab and collaborating institutions, and acknowledge support from the DOE and NSF (USA); CEA and CNRS/IN2P3 (France); FASI, Rosatom and RFBR (Russia); CAPES, CNPq, FAPERJ, FAPESP and FUNDUNESP (Brazil); DAE and DST (India); Colciencias (Colombia); CONACyT (Mexico); KRF (Korea); CONICET and UBACyT (Argentina); FOM (The Netherlands); PPARC (United Kingdom); MSMT (Czech Republic); CRC Program, CFI, NSERC and WestGrid Project (Canada); BMBF and DFG (Germany); SFI (Ireland); Research Corporation, Alexander von Humboldt Foundation, and the Marie Curie Program.

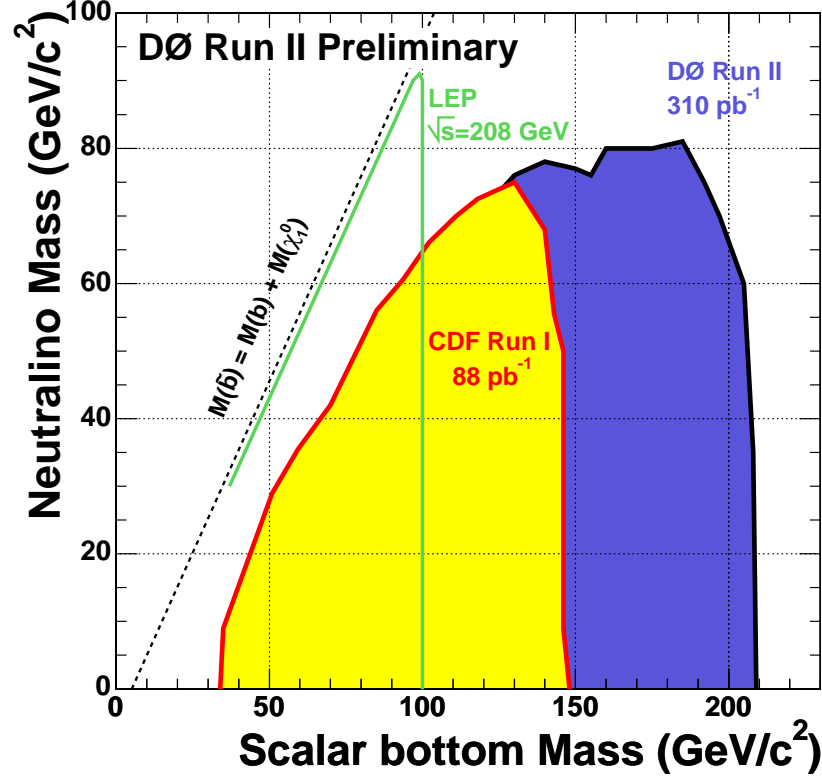


FIG. 6: 95% CL exclusion contour, after all selections, including single  $b$  tagging and combining the 3 sets of cutoffs in  $\cancel{E}_T$  and jet  $p_T$  described in section VIII.

- 
- [1] DØ Collaboration, V. Abazov *et al.*, “The Upgraded DØ Detector,” in preparation for submission to Nucl. Instrum. Meth. Phys. Res. A.
  - [2] The coordinates used are  $z$  which runs along the beam,  $\phi$  the azimuthal angle around the beam and  $\theta$  the angle w.r.t. to the beam. Pseudo-rapidity  $\eta$  is used in place of  $\theta$  and is defined as  $\eta = -\ln(\tan \frac{\theta}{2})$ .
  - [3] T. Sjöstrand *et al.*, “PYTHIA 6.2 Physics and Manual”.  
<http://arxiv.org/abs/hep-ph/0108264>
  - [4] H.L. Lai [CTEQ Collaboration] Eur. Phys. J. C 12 (2000) 375 [hep-ph/9903282].
  - [5] S. Agostinelli *et al.*, NIM A 506 (2003), 250-303.
  - [6] <http://pheno.physics.wisc.edu/~plehn/prospino/prospino.html>  
W. Beenakker, R. Hoepker, and M. Spira hep-ph/9611232  
“PROSPINO: A Program for the Production of Supersymmetric Particles in Next-to-leading Order QCD”.
  - [7] M.L. Mangano *et al.*,  
“ALPGEN, a generator for hard multiparton process in hadronic collisions”  
JHEP 0307 (2003) 001.
  - [8] John Campbell and Keith Ellis  
MCFM - Monte Carlo for FeMtobarn processes.  
<http://mcfm.fnal.gov/>
  - [9] N. Kidonakis and R. Vogt, “Top quark production at the Tevatron at NNLO”  
Eur.Phys.J. C33 (2004) S466-S468.
  - [10] T. Junk, “Confidence Level Computation for Combining Searches with Small Statistics”  
NIM A434, p. 435-443, 1999.